NASA TECHNICAL NOTE

NASA TN D-3132

NASA TN D-3132

OPTIMUM DESIGN OF MAGNETIC BRAKING COILS WITH SPECIAL APPLICATION TO LEWIS DROP TOWER EXPERIMENTS

by H. G. Kosmahl
Lewis Research Center
Cleveland, Ohio

NATIONAL AERONAUTICS AND SPACE ADMINISTRATION • WASHINGTON, D. C. • DECEMBER 1965

NASA TN D-3132

OPTIMUM DESIGN OF MAGNETIC BRAKING COILS WITH SPECIAL APPLICATION TO LEWIS DROP TOWER EXPERIMENTS

By H. G. Kosmahl

Lewis Research Center
Cleveland, Ohio

NATIONAL AERONAUTICS AND SPACE ADMINISTRATION

For sale by the Clearinghouse for Federal Scientific and Technical Information
Springfield, Virginia 22151 – Price $1.00

OPTIMUM DESIGN OF MAGNETIC BRAKING COILS WITH SPECIAL APPLICATION TO LEWIS DROP TOWER EXPERIMENTS

by H. G. Kosmahl

Lewis Research Center

SUMMARY

General analytical treatment of a design of magnetic braking coils and magnetic braking action is given. However, numerical results are computed and tabulated only for the specific application and requirements of the Lewis Research Center (400-ft) drop facility.

A method for calculating the mutual inductance of unconventionally wound coils has been developed. Braking action has been computed for the case of a primary coil used to stop the motion of a secondary coil moving along the common axis and with a given mass and initial kinetic energy. The energy required in the primary coil can be minimized. The amount of deceleration can be adjusted by varying only the primary voltage (current). The preceding tasks may be accomplished with a primary system requiring a minimum number of turns.

For the specific case of a freely falling payload in the Lewis 400-foot drop facility, weighing 1000 kilograms and having a final velocity of 50 meters per second, a primary power of between 10 to 20 megawatts associated with a primary current of about 100 kiloamperes is required for 10 seconds to stop the payload with a deceleration equal to or less than 30 g's. The corresponding primary magnetic field is of the order of 1 Weber per square meter (10 000 gauss).

A primary coil with a linearly increasing winding density has been found to require the least energy for a given maximum deceleration. Because of the nonlinear nature of the equations involved, additional computations may be necessary for numerical cases not tabulated in this paper. For the same reason, a closed form optimization procedure is not feasible.

INTRODUCTION

The use of magnetic brakes in many industrial and scientific applications is a well established practice. The mechanism of operation can be best explained from Lenz's law which says that magnetic fields induced in one circuit as a result of interaction with another circuit oppose each other.

The purpose of the present investigation is to find a configuration of a primary magnetic coil (in the following coil 1) and of a secondary coil 2 such that the motion of coil 2 through fields of coil 1 can be brought to a stop under controlled conditions requiring minimum primary energy. For the particular application being considered herein (i. e., the drop experiments in Lewis Research Center zero-gravity drop tower facility) the payload falling freely through a height of 120 meters approaches a speed of about 50 meters per second. It must be decelerated to almost a perfect stop with the deceleration not to exceed a specified maximum. The solution of this and other similar problems requires the knowledge of the mutual inductance M between two unconventionally wound circuits as functions of distance between them. (Symbols are defined in appendix A.) The determination of M (appendix B) was accomplished by expanding a number of winding density functions (winding schemes) in a complex Fourier integral and applying them to a Bessel integral expansion of the vector potential. From the latter the mutual inductance and the self inductance can be determined.

The circuit equations as well as the equation of motion of the payload in magnetic and gravitational fields are then solved on a computer and an optimization of the coil system with respect to minimum energy and minimum size is carried out.

The significance of these results lies in the possibility of designing a system requiring a minimum of primary energy, in which the braking action is accomplished in a precisely adjustable manner with respect to the desired degree of deceleration by simply varying the voltage of the primary circuit and/or the length of the primary coil.

ANALYSIS OF MAGNETIC DECELERATION

The interaction of two, predominantally magnetically coupled coils can be best described by their mutual inductance M. Figure 1 shows two magnetic coils denoted by subscripts 1 and 2. Coil 1 is connected to a power source with the load voltage V_o and an impedance $R_g \ll R_1$. The origin of the coordinate system $z = 0$ represents the (physical) end of coil 1, the latter being immobile. Coil 2 is short circuited and is assumed to move only in the z-direction, which points in the direction of the earth's gravitation.

A magnetically noninteracting mass m_o is affixed rigidly to the turns of coil 2. The latter has a mass m_2 so that $m = m_o + m_2$ represents the full mass of the second coil. Suppose that a steady-state current $i_{1,0}$ flows in coil 1 prior to any interaction with coil 2. If the latter is permitted to fall in the negative z-direction due to gravitational force and its momentary distance from $z = 0$ is z, the following equations are applicable to determine the instantaneous velocity $\dot{z}\left[z(t)\right]$ of the second coil:

$$V_o = i_1(t)R_1 + L_1 \frac{di_1}{dt} + \frac{dM(z)}{dt} i_2 + M(z) \frac{di_2}{dt} \tag{1}$$

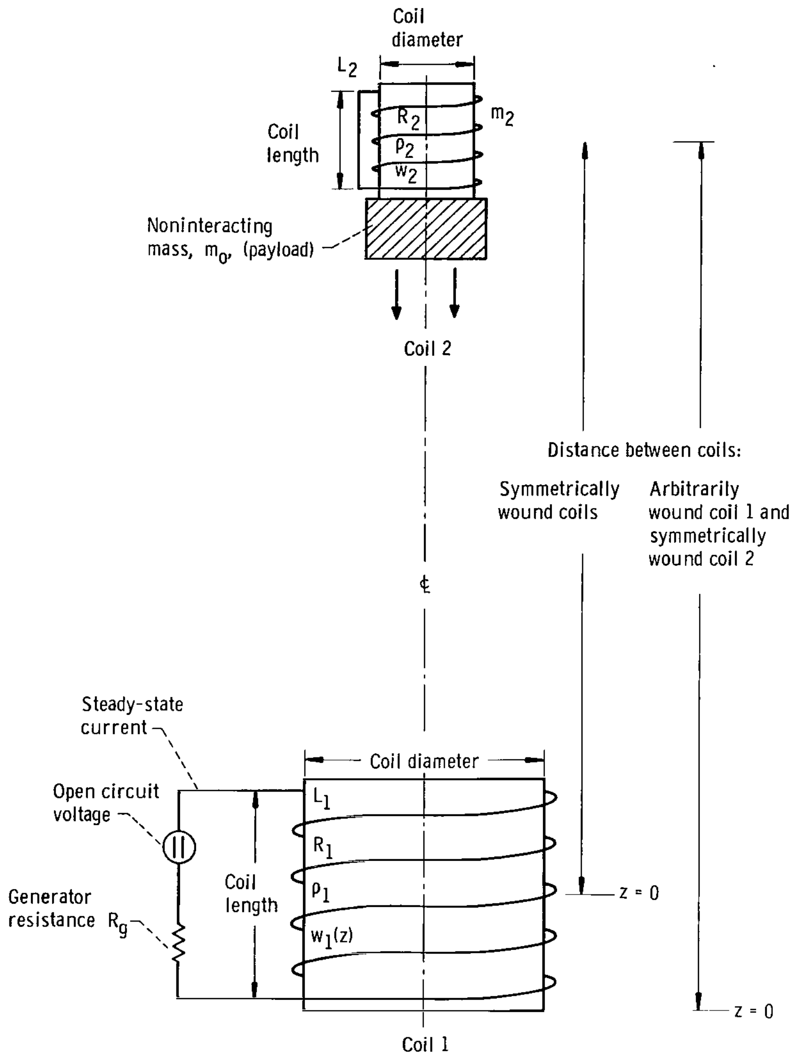

Figure 1. - Schematic arrangement of coils 1 and 2 for falling payload.

$$0 = i_2(t)R_2 + L_2 \frac{di_2}{dt} + \frac{dM(z)}{dt} i_1(t) + M(z) \frac{di_1(t)}{dt} \tag{2}$$

The repelling magnetic force F_m acting upon the turns of the falling payload is

$$F_m = i_1(t)i_2(t) \frac{\partial M(z)}{\partial z} \tag{3}$$

where z is the distance between defined points in coils 1 and 2. The equation of motion of the payload is

$$\ddot{z} = g - \frac{i_1(t)i_2(t)}{m} \frac{\partial M(z)}{\partial z} \tag{4}$$

Multiplication by $\dot{z}$ and integration between $t = 0$ and $t = t$ (fig. 1) result in the energy equation

$$\dot{z}^2(t) = 2g\left[h - z(t)\right] - \frac{2}{m}\int_{t=0}^{t=t} i_1(t) \cdot i_2(t) \frac{\partial M(z)}{\partial z} \dot{z}(t)dt \tag{5}$$

since $\dot{z}(0)$, the velocity at $z = h$, is zero. The initial value conditions are $i_1(0) = i_0$ and $i_2(0) = 0$. After $M = M(z)$ has been computed with the help of relations derived in appendix B, equations (1), (2), and (5) are solved simultaneously for $z(t)$ and $\dot{z}(t)$. The values $\dot{z}(t_s) = 0$ and $z(t_s)$ give the stopping time t_s and the stopping position $z(t_s) = x_s$ of the payload. The total output of computer data contained the currents i_1 and i_2, $M[z(t)]$ and $\partial M[z(t)]/\partial z(t)$, the normalized force $G = (i_1 i_2\ \partial M/\partial z)/mg$, the inductances L_1 and L_2, the resistances R_1 and R_2 that have been computed as functions of the coil diameters 2a and 2b, wire diameters d_1 and d_2, the winding density w_1 and w_2, the coil lengths l_1 and l_2, and the specific resistivities ρ_1 and ρ_2 of the coil wires.

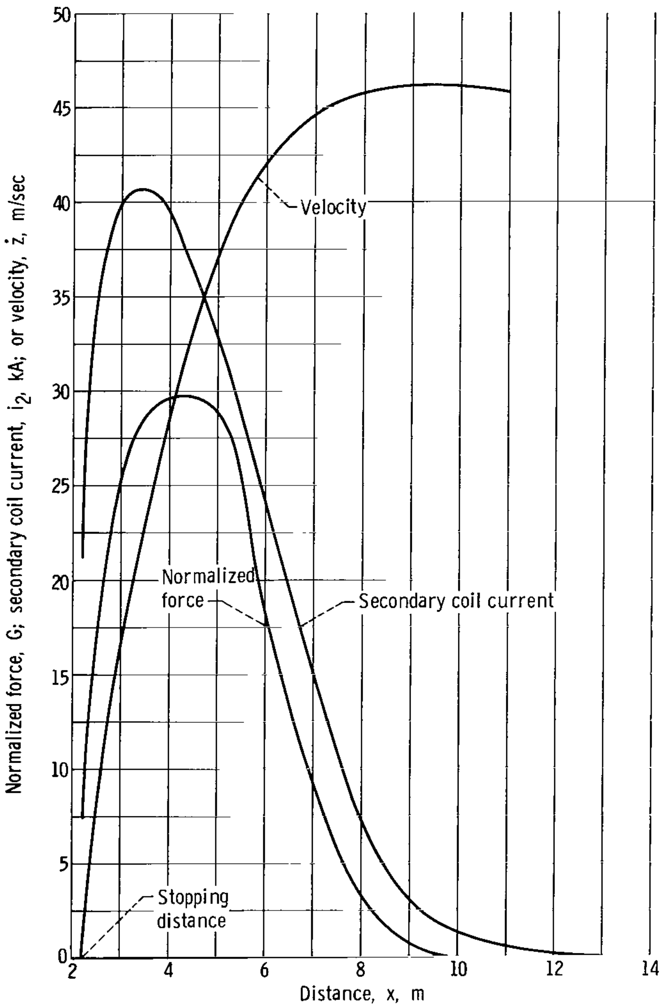

Figure 2. - Typical plots of velocity, secondary current, and normalized force against distance between coils. Winding density, $w_1 = 8\left(1 - \frac{z}{8}\right)$.

Notice that the decelerating force persists even after $\dot{z}$ has reached zero (fig. 2) because the time constant $\tau_2 = L_2/R_2$ prevents an instantaneous decay of i_2 to zero. Thus, F_m remains finite over a period of a few constants, and a "perfect" stop is possible.

A payload m_0 of 900 kilograms has been assumed to which the mass of aluminum turns affixed to the payload has been added. Because of specific requirements the diameter of the primary coil has been kept constant at $2a = 3$ meters. The primary turns consisted of 0.1-meter-diameter copper wire throughout with a specific resistivity of $1.8\times10^{-8}(\Omega)(m)$.

DISCUSSION OF RESULTS

The more important computer results have been presented in table I. In addition to geometrical parameters they contain the primary coil voltage V_1, the steady-state primary current $i_{1,0}$ at the beginning of interaction, the power P, the normalized force G in multiples of g, and the position x_s at which the center of the payload turns approaches zero velocity, measured from the bottom end of the primary coil $z = 0$. Also listed are two values of the specific resistivity ρ_2 for aluminum which have been assumed to be 3×10^{-8} $(\Omega)(m)$ at room temperature $T = 300^\circ$ K and 0.6×10^{-8} $(\Omega)(m)$ at $T = 80^\circ$ K (liquid nitrogen (unpublished data, obtained by John C. Fakan of Lewis, show values as low as $0.3\times10^{-8}(\Omega)(m)$). It should be noted that the primary current i_1 is not absolutely constant; however, because of the relatively large time constant τ_1, the current i_1 changes by less than 10 percent of the initial $i_{1,0}$ value.

The maximum temperature rise in the secondary turns was less than 25° C, with an average of approximately 10° C, rendering this effect entirely unimportant.

Table I refers to three different winding schemes. For deciding which scheme is preferable over the others the primary power must not be the sole criterion because of the presence of restraining conditions and ease of construction. Two important conditions in drop tower applications are: the time constant τ_1 to be as small as possible in order for the current i_1 to build up as close to its final value $i_{1,0}$ as possible in a time $t \leq 10$ seconds. The latter number is approximately twice the free fall time through a height h equal to 120 meters, the time $t = 10$ seconds being the maximum period available for the buildup of current in case of a two way "up and down" experiment.

The other conditions for the Lewis Research Center drop tower experiments is the upper limit of deceleration G to be smaller than 30 g's. The computations show clearly that the power requirements to bring about a full stop could be reduced substantially if the condition $G \leq 30$ were disregarded because stopping action could then be accomplished with a shorter primary coil.

An evaluation of the tables leads to the following important conclusions:

(a) Application of liquid-nitrogen cooling to the secondary turns reduces substantially (50 to 70 percent) primary power requirements in the case of $d_2 = 0.05$ meter and only slightly (about 15 percent) in the case of $d_2 = 0.1$ meter for the assumed value of specific resistivity.

(b) Primary power requirement decreases rapidly as b is increased (while keeping $a = 1.5$ m constant) from 0.75 to 1.0 meter.

TABLE I. - COMPUTER RESULTS AND COIL PARAMETERS

[Primary coil radius, 1.5m; primary coil specific resistivity, 1.8×10^{-8} (Ω)(m); primary coil conductor diameter, 0.1m.]

Primary coil length, l_1, m	Secondary coil conductor diameter, d_2, m	Secondary coil specific resistivity, ρ_2, (Ω)(m)	Secondary coil winding density, w, turns/m	Secondary coil radius, b, m	Secondary coil length, l_2, m	Primary coil voltage V_1, V	Initial current, $i_{1,0}$ kA	Maximum normalized force, G_{max}, g	Stopping distance, x_s, m	Power, P, MW	Primary coil time constant, τ_1, sec
Primary coil winding density, $10\left(1 - \frac{z}{l_1}\right)$											
8	0.05	3.0×10^8	6	1.00	0.6	107	123.8	29.8	0.65	13.3	2.3
8	.10	3.0		1.00		98	113.4	30.2	1.96	11.1	
8	.10	.6		1.00		91	105.3	30.3	1.87	9.6	
8	.05	.6		.75		124	144.0	30.2	2.20	17.8	
8	.10	3.0				141	163.2	29.6	2.10	23.0	
8	.10				.7	138	159.7	29.5	1.93	22.0	
8	.05				.8	146	169.0	29.7	.06	24.7	
8	.10				.8	135	156.0	29.8	.10	21.1	
8	.10				1.0	131	151.0	29.8	1.90	19.9	
8	.10				1.2	128	148.2	30.0	1.95	19.0	
8	.10				1.6	125	144.7	31.0	2.20	18.1	
12	.05	.6			.6	170	131.0	19.2	1.2	22.4	3.55
12	.05	3.0			.6	237	183.0	19.8	.85	43.3	3.55
8	.10		2		1.2	123	142.0	29.5	1.80	17.5	2.3
8	.10		4		1.2	122	141.0	29.6	1.90	17.2	2.3
8	.10		6		1.2	128	148.0	29.8	1.95	18.9	2.3
8	.10		8		1.2	135	156.0	30.2	2.10	21.1	2.3
Primary coil winding density, $2\left(1 + 5 \cos \frac{\pi z}{l_1}\right)$											
8	0.05	0.6×10^8	6	0.75	0.6	134	93.0	39.0	4.5	12.5	3.46
8	.05	3.0				170	119.0	44.1	5.0	20.0	3.46
8	.10	.6				149	103.0	41.3	4.9	15.5	3.46
12	.05	.6				191	88.0	27.0	7.0	16.8	3.65
12	.05	3.0				257	119.0	32.0	7.8	30.6	3.65
12	.10	.6				201	93.0	26.0	6.7	18.7	3.65
Primary coil winding density, $2\left[1 + 5\left(1 - \frac{\lvert 2z \rvert}{l_1}\right)\right]$											
12	0.05	0.6×10^8	6	0.75	0.6	175	96.4	27.6	6.9	16.9	3.22
12	.1	.6	6	.75	.6	185	102.0	27.7	6.8	18.9	3.22
12	.05	3.0	6	.75	.6	232	127.6	29.6	7.6	29.6	3.22
12	.1	3.0	6	.75	.6	201	110.5	27.3	6.9	22.2	3.22

(c) For equal values ρ_2, d_2, l_2, w_2, and b, respectively, while keeping $G \leq 30$, the power requirements of the three tabulated winding schemes necessary to bring about a full stop are about the same. (The energy requirements, however, are not equal.)

(d) The winding scheme $w_1 = \text{const}[1 - (z/l)]$ produces the shortest time constant $\tau_1 = 2.3$ seconds and requires the smallest number of turns to bring about a "full stop" of the payload.

The meaning of full stop, as used herein, refers to a motion in which the velocity decays directly to zero, without oscillations in the sign of the deceleration (i.e., no acceleration). Notice that the position of stop x_s in all symmetrically wound coils lies above the coil center $z = l_1/2$. This happens because in symmetric coils the mutual inductance M has a maximum and $\partial M/\partial z = 0$ at the center of the coil. Thus $\partial M/\partial z$ reverses its sign in going through the center. Now, in the expression for the force (eq. (3)), $i_1(t)$ remains almost constant and the sign of i_2 depends mainly on that of $\partial M/\partial z$. Because the time constant τ_2 is rarely below 0.1 second in this particular design, a reversal in the sign of $\partial M/\partial z$ in going through the center would precede that occurring in i_2. Therefore, if the payload moved over the center, a short period of acceleration would follow: the payload velocity would increase temporarily before final deceleration could occur to cause the final stop. Such a "two phase" deceleration with a short acceleration period in between has been examined on the computer and seems to produce a workable mode of operation requiring approximately 10 percent less power than "one phase" stopping. The evaluation of the "two phase" cases, however, is more ambiguous than that of "one phase" stopping and has not been considered in this discussion.

The effect of changing l_2 on the power requirements indicates an optimum length $l_2 < l_1$. This result is easily explained by the fact that two competing factors produce a minimum power requirement: increasing l_2 increases the flux through the secondary and, therefore, the braking force. On the other hand the mass m_2 increases proportionally with l_2 and reduces the effect of the decelerating force in front of the integral (eq. (5)).

The highest computed value l_2 is $l_2 = 3.6$ meters at which number the primary power requirement is still decreasing slightly; however, the dependence of P against l_2 flattens out and an increase of power requirements with increasing l_2 is likely to occur at some large value of l_2, which is of little practical interest to the desired application.

A clear dip in power requirements appears if w_2 is changed, as can be seen from table I. This optimum occurs because of the competing effects between the secondary time constant τ_2 which prevents a rapid build-up of i_2 and of the mutual inductance $M_{1,2}$. Since both τ_2 as well as $M_{1,2}$ increase with increasing w_2, a minimum in the required power occurs if the total interaction time is not substantially larger than τ_2.

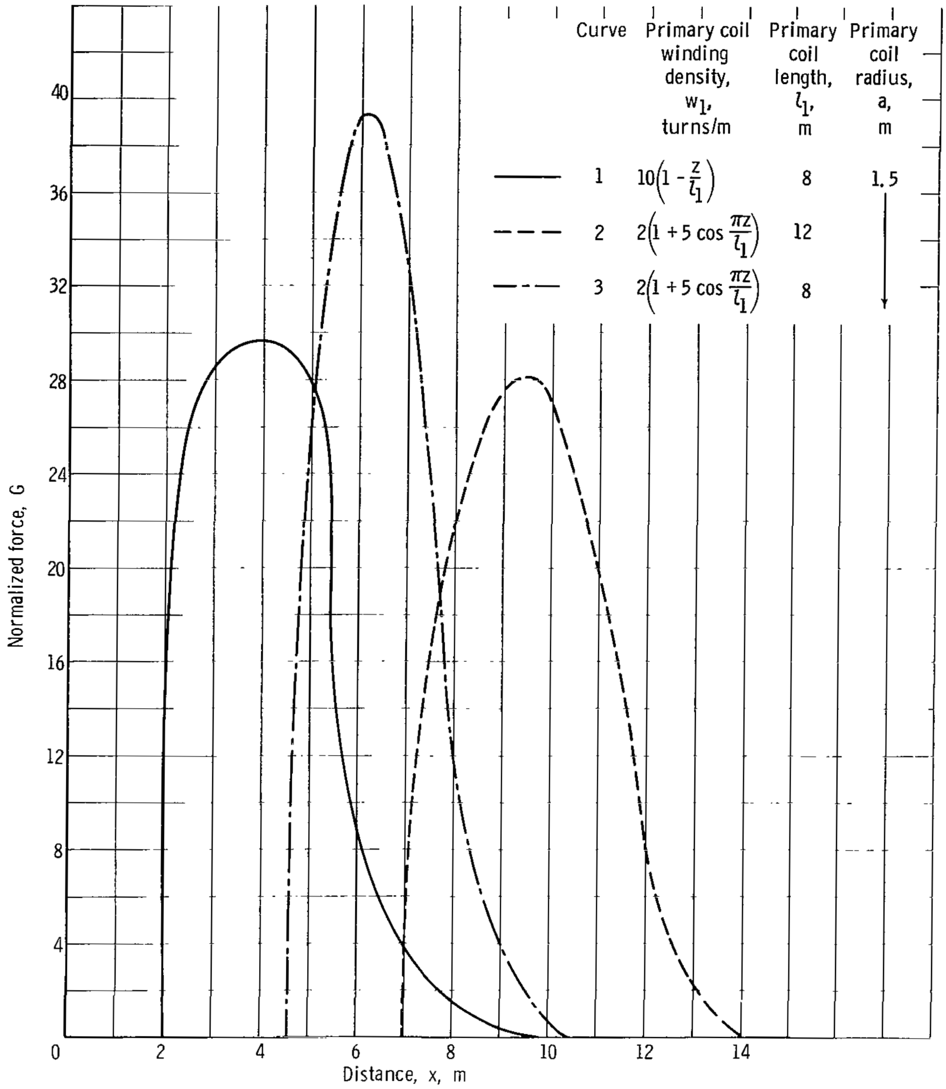

Figure 3. - Normalized force against distance for three different winding schemes. Secondary coil winding density, 6 turns per meter; secondary coil length, 0.6 meter; secondary coil radius, 0.75 meter.

Because of the approximate constancy of i_1 the primary energy requirement is proportional to $i_1^2\tau_b$, where τ_b is the braking time. The smallest braking time is accomplished with a steplike-shaped deceleration of maximum permissible amount over the time τ_b and which is zero elsewhere. Figure 3 shows the normalized magnetic deceleration G against distance for two different geometries. The length of coil 1 wound according to $w_1 = 10(1 - z/l_1)$ is $l_1 = 8$ meter; that of coil 2 wound according to $w_1 = 2(1 + 5\cos \pi z/l_1)$ is $l_1 = 12$ meter. The difference in coil length is necessary in order not to exceed G = 30, as may be seen from comparing curves 2 and 3 in figure 3. A comparison of the curves shows that curve 1 except for the exponentiallike tail, more closely approaches the steplike function than curves 2 and 3. The latter resemble rather resonancelike curves.

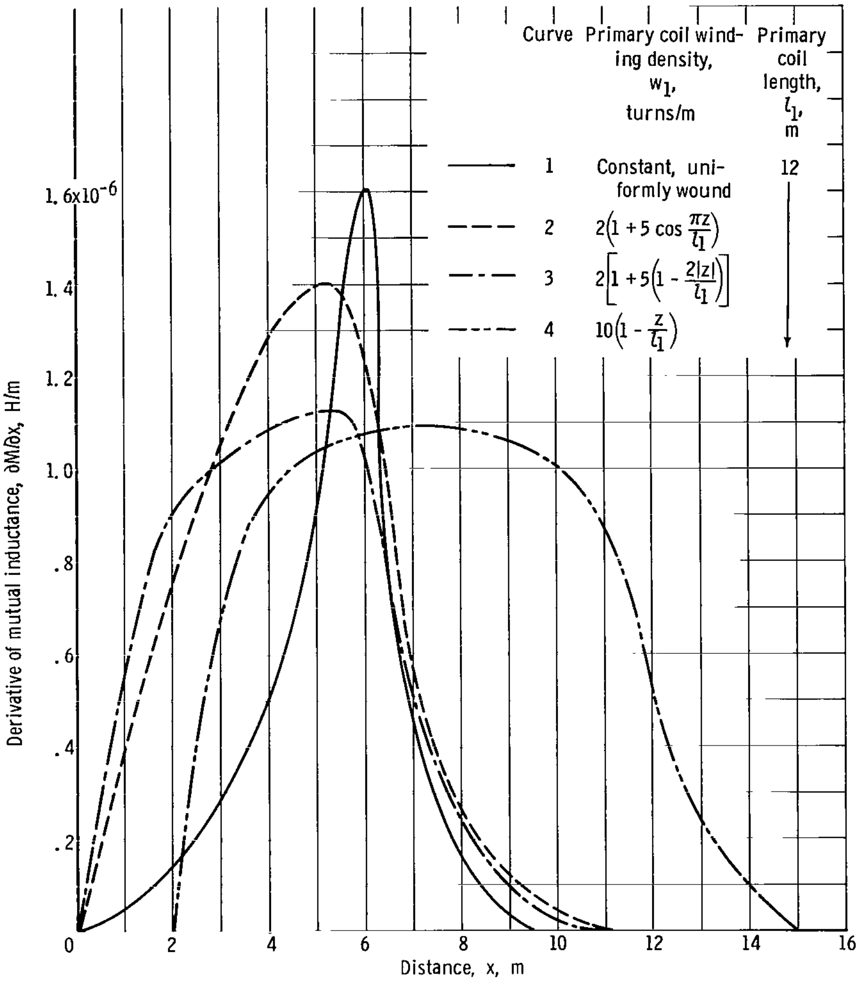

Figure 4. - Derivative of mutual inductance against distance for four different winding schemes. Secondary coil winding density, 6 turns per meter; secondary coil length, 0.6 meter; secondary coil radius, 0.75 meter.

Figure 4 shows $\partial M/\partial x$ against x for a variety of winding schemes; x is the distance from the center of coil 2 to the center of coil 1 in symmetrically wound primary coils and from center of coil 2 to the remote end of coil 1 for the winding scheme $w_1 = 10[1 - (z/l_1)]$. A uniformly wound solenoid produces the narrowest, the $1 - (z/l_1)$ winding scheme the closest to rectangular or steplike shape. Figure 4 shows that $\partial M/\partial x$ is much wider than the deceleration G in figure 3. Both are plotted on the same scale of x. This behavior results from the existence of a time constant τ_2 which is not substantially smaller than the braking time τ_b. Thus, there is a delay before the maximum of i_2 can develop and the width of G is shortened (fig. 2).

Figure 5 shows P_1, τ_1, G_{max} and the primary number of ampere turns plotted as functions of $w_{1,0}$ for the winding density $w_1 = w_{1,0}[1 - (z/l_1)]$. As $w_{1,0}$ increases the power necessary to produce a full stop, P_1 decreases over the examined range. On

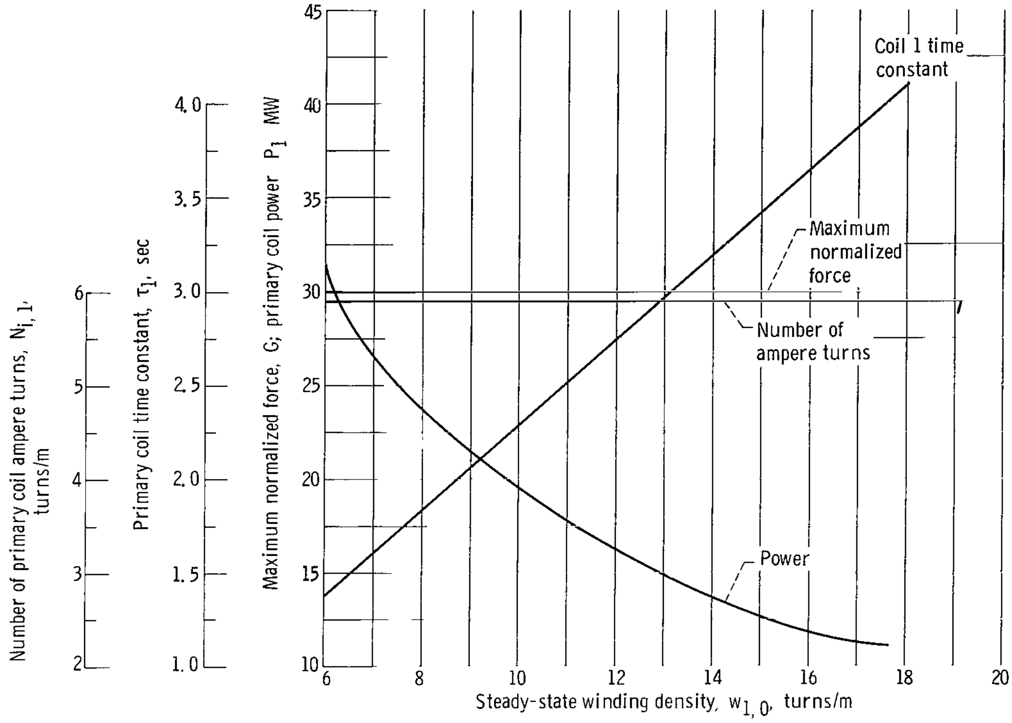

Figure 5. - Power, time constant, normalized force, and number of ampere turns as functions of steady-state winding density for primary winding density required to stop payload. Primary coil length, 8 meters. Secondary coil parameters: winding density, 6 turns per meter; coil length, 1.2 meters; coil conductor diameter, 0.1 meter; specific resistivity, 3×10^{-8} (Ω)(m).

the other hand G_{max} remains constant (G_{max} = 30g) as does the total number of ampere turns

$$i_1 \int_0^{l_1} w_{1,0}\left(1 - \frac{z}{l_1}\right)dz$$

It can, therefore, be concluded that as long as l_1 and the total number of ampere turns are kept constant G_{max} will not change.

A practical limitation in the reduction of P_1 is twofold: the increase in τ_1 (which could be irrelevant in other cases) and the necessity to increase the radius of the turns. Also, at some point the change in i_1 must be considered, and the integral

$$\int V_1 i_1(t)dt$$

must be used for primary energy calculations. The power curve P_1 in figure 5 flattens out. Its minimum lies beyond the range τ_1 which is of interest for the considered applications.

Figure 2 (p. 4) is a plot of the velocity $\dot{z}$, the secondary current i_2, and the force G against x. Note that at $x = x_s$ the payload comes to a stop (i.e., $\dot{z} = 0$), but both i_2 and G are different from zero, which makes a perfect stop possible. The shape of G follows closely that of i_2. Because of the constancy of i_1 this is only possible if $\partial M/\partial x$ remains approximately constant, in agreement with curve 4 in figure 4.

CONCLUDING REMARKS

A design of a magnetic coil system in applications as a magnetic brake has been investigated and a method for calculating the mutual inductance and self-inductance of nonconventionally wound coils has been developed. The main features of this brake are minimum primary energy requirement to bring to a stop a payload with a given initial kinetic energy, production of a smooth deceleration in a steplike function with the degree of deceleration being easily adjustable by changing only the primary voltage and/or primary coil length l_1, accomplishment of the preceding tasks with a primary coil having as few turns as possible, and a required flux density equal to about 1 Weber per meter squared (10 000 gauss).

A very definite optimum design has been determined under the imposed restrictive conditions (i.e., maximum deceleration and coil diameter ratio). The choice of parameters for minimum power requirement is generally noncritical; however, deviations of a factor of 2 in some of the parameters from their optimum value may render the system infeasible.

It is concluded that an elegant, efficient, and reliable system could be developed unless stability studies, not carried out in the frame of this investigation, produced information to the contrary.

Although not discussed herein, it is conceivable that an electromagnetic system could be designed to fulfill the double purpose of launching and stopping the payload within the very same coil, thus eliminating the need for mechanical launching guns.

Lewis Research Center,
National Aeronautics and Space Administration,
Cleveland, Ohio, September 9, 1965.

APPENDIX A

SYMBOLS

A_φ	azimuthal component of vector potential $\vec{A}$
a	radius of primary coil, m
B	magnetic flux density, Wb/m^2
b	radius of secondary coil, m
C, D	general constants
C(k)	wave number dependent parameter
d	distance between coils, m
dS	surface element
ds	line element
F_m	magnetic force
G	normalized magnetic force, F/mg
g	9.81 m/sec^2
H	magnetic field strength, A/m
h	height, m
$I_n(kr)$	modified Bessel function of first kind n^{th} order and argument kr
$\mathcal{I}$	current, A
j	current per unit length, A/m
$K_n(kr)$	modified Bessel function of second kind, n^{th} order and argument kr
k	Fourier integral wave number
L	self inductance, H
l	length of coil, m
M	mutual inductance between coils 1 and 2, H
m	mass, kg
N	number of turns
P	power, W
R	resistance, Ω
r	radius, m
S(k)	Fourier amplitude function
t	time, sec
V	voltage, V
w	winding density, turns/m
x	distance, m
z	axial coordinate
$\alpha(k)$, $\Phi(k)$	phase angle
δ	Dirac's delta function
ρ	specific resistivity, (Ω)(m)
μ	permeability
μ_o	$4\pi \times 10^{-7}$ H/m
τ	time constant, L/R
τ_b	breaking time

Subscripts:

e	external
i	internal
max	maximum

s	stopping
φ	azimuthal
0	initial
1	primary coil (coil 1)
2	secondary coil (coil 2)

Superscripts:

$\vec{}$	vector
$\dot{}$	first derivative
$\ddot{}$	second derivative

APPENDIX B

DERIVATION OF EXPRESSIONS FOR MUTUAL INDUCTANCE AND SELF-INDUCTANCE OF COILS WITH CYLINDRICAL SYMMETRY

If it is assumed that the current sheet has a negligible thickness and circulates only in the azimuthal direction φ at $r = r_o$, only one component A_φ of the vector potential will exist. This can be accomplished by applying a suitable winding technique or current feeding technique.

For a coil of radius r_o the latter may be represented by references 1 and 2.

$$A_{\varphi, i} = \int_{-\infty}^{+\infty} C_i(k) I_1(kr) e^{i[kz+\alpha(k)]} dk \qquad \text{for } r < r_o \tag{B1}$$

$$A_{\varphi, e} = \int_{-\infty}^{+\infty} C_e(k) K_1(kr) e^{i[kz+\alpha(k)]} dk \qquad \text{for } r > r_o \tag{B2}$$

The boundary conditions for B and H on the interface $r = r_o$ between the internal and external region, denoted by subscripts i and e, respectively, are

$$A_{\varphi, i} = A_{\varphi, e} \; (B_i = B_e) \tag{B3}$$

and

$$\frac{1}{\mu_i} \frac{1}{r} \frac{\partial}{\partial r}\left(rA_{\varphi, i}\right) - \frac{1}{\mu_e} \frac{1}{r} \frac{\partial}{\partial r}\left(rA_{\varphi, e}\right) = j_{s, \varphi}(z) \qquad \text{at} \quad r=r_o \tag{B4}$$

where $j_{s, \varphi}(z)$ is the surface current density per unit length

$$j_{s, \varphi}(z) = f(z)\delta(r - r_o) \qquad \text{for } 0 < z < l$$

and $j_{s, \varphi}(z) = 0$ elsewhere. If only the winding density $w(z)$ but not the current $\mathcal{I}$ in the turns is a function of z, the following expansion of j_φ is appropriate:

$$j_\varphi = \mathcal{J} w(z) = \mathcal{J} w_1 \int_{-\infty}^{\infty} S(k) e^{ikz} dk = \mathcal{J} w_1 \int_{-\infty}^{\infty} |S(k)| e^{i[(kz+\Phi(k)]} dk \tag{B5}$$

$$S(k) = \frac{1}{2\pi} \int_{-\infty}^{\infty} e^{-ikz} w(z) dz = |S(k)| e^{i\Phi(k)} \tag{B6}$$

From expressions (B4) to (B6) the following equation is obtained for $\mu_i = \mu_e = \mu_o$

$$\int_{-\infty}^{\infty} \left\{ \frac{C_i(k) \frac{\partial}{\partial r} [rI_1(kr)] - C_e(k) \frac{\partial}{\partial r} [rK_1(kr)]}{r} \right\}_{r=r_o} e^{i[kz+\alpha(k)]} dk$$

$$= \int_{-\infty}^{\infty} \left[C_i(k) k I_o(kr_o) + C_e(k) \cdot kK_o(kr_o) \right] e^{i[kz+\alpha(k)]} dk$$

$$= \mu_o j_\varphi(z) = \mu w_1 \mathcal{J} \int_{-\infty}^{\infty} |S(k)| e^{i[kz+\Phi(k)]} dk$$

$$= 2\mu_o w_1 \mathcal{J} \int_0^{\infty} |S(k)| \cos\left[kZ + \Phi(k)\right] dk \tag{B7}$$

because the integration over sin from $-\infty$ to ∞ is zero. Equations (B3) and (B4) can be satisfied only if

$$\alpha(k) = \Phi(k) \tag{B8}$$

$$C_i(k)I_1(kr_o) - C_e(k)K_1(kr_o) = 0 \tag{B9}$$

$$C_i(k)I_o(kr_o) + C_e(k)K_o(kr_o) = \frac{\mu_o \mathcal{J} w_1}{k} \left| S(k) \right| \tag{B10}$$

With

$$I_o(kr)K_1(kr) + I_1(kr)K_o(kr) \equiv \frac{1}{kr}$$

the constants C_i and C_e are determined from (B9) and (B10) to

$$C_i(k) = \mu_o \mathcal{J} w_1 \left| S(k) \right| r_o K_1(kr_o) \tag{B11}$$

$$C_e(k) = \mu_o \mathcal{J} w_1 \left| S(k) \right| r_o I_1(kr_o) \tag{B12}$$

Thus, the expressions for the vector potential (B1) and (B2) may be written

$$A_{\varphi, i} = 2\mu_o r_o \mathcal{J} w_1 \int_0^\infty \left| S(k) \right| K_1(kr_o)I_1(kr)\cos[kz + \Phi(k)]\, dk \tag{B13}$$

and, similarly,

$$A_{\varphi, e} = 2\mu_o r_o \mathcal{J} w_1 \int_0^\infty \left| S(k) \right| I_1(kr_o)K_1(kr)\cos[kz + \Phi(k)]\, dk \tag{B14}$$

Mutual Inductance Between Two Coils

Now the relation (B13) and (B14) is applied to calculate the mutual inductance M between coils 1 and 2, each having a constant diameter 2a and 2b, respectively. In addition, the winding density on the second coil is assumed constant (e. g., w_2 = const) even though this restriction is not, generally, necessary.

In a distance between z and $z + dz$, counted from a fixed point $z = 0$ in the primary coil (subscript 1), there will be $w_2\,dz$ turns of secondary coil (subscript 2). Thus, the mutual inductance between the element $w_2\,dz$ and the entire flux coming out of the primary coil is

$$dM = w_2\ dz \int_{S_2} \vec{B}_1(z)_{r=b} \cdot \vec{n}\ dS_2 = w_2\ dz \oint_{s_2} \vec{A}_1(z)_{r=b}\ \vec{ds}_2 \tag{B15}$$

where S_2 and s_2 designate the area and the length element of turns in the secondary coil, respectively. Because $A_1(z)$ is constant over the azimuth at a given radius, the following may be written for dM

$$dM = 2\pi b\ A_{1,\varphi}(z)_{r=b}\ w_2\ dz \tag{B16}$$

The integration (B16) over the entire length l_2 results in

$$M = 4\mu_0 abw_1 w_2 \pi \int_{k=0}^{\infty} dk \int_{z=d-(l_2/2)}^{d+(l_2/2)} |S(k)|\,K_1(ka)I_1(kb)\cos\left[kz + \Phi(k)\right] dz \tag{B17}$$

where d is the distance between a fixed point in coil 1 and the center of coil 2.

Self-Inductance of Coil

The relations developed for calculating M will now be applied to determine the self-inductances of axially symmetrical coils of constant diameter. This is done by first finding the flux linking any turn and then integrating over all turns.

Modifying equation (B15) to apply to the very same coil yields

$$L = \int_{l_1} w_1(z)dz \int_{S_1} \vec{B}_1(z)_{r=a}\, d\vec{S}_1$$

$$= \int_{l_1} w_1(z)dz \oint \vec{A}_1(z)_{r=a}\, d\vec{s}_1$$

$$= 2\pi a \int_{l_1} w_1(z) A_{1,\varphi}(z)_{r=a}\, dz \tag{B18}$$

Fourier Integral Expansion of $w_1(z)$

The function

$$w_1(z) = f(z)\delta(r - r_o)$$

for either

$$f(z) \neq 0 \text{ in } 0 < z < l_1, \text{ or } f(z) \neq 0 \text{ in } -\frac{l}{2} < z < \frac{l}{2}$$

and

$$f(z) \equiv 0 \text{ elsewhere}$$

will be expanded in a Fourier integral:

$$f(z) = \int_{-\infty}^{\infty} S(k)e^{ikz}\, dk$$

Note in the following that the center of expansion $z = 0$ coincides with the center of coil 1 for symmetrically wound coils and with the bottom of coil 1 in all other cases, in agreement with figure 1. The distance x is always counted from the proper center of expansion on coil 1 to the center of coil 2.

$$
\left.
\begin{aligned}
w_1(z) &= \begin{cases} \text{const} & \text{for } -\dfrac{l}{2} < z < \dfrac{l}{2} \\ 0 & \text{elsewhere} \end{cases} \\
S(k) &= \frac{\text{const}}{2\pi} \int_{-l/2}^{l/2} e^{-ikz}\, dz \\
&= \text{const} \frac{1}{\pi k} \sin \frac{kl}{2}
\end{aligned}
\right\}
\tag{B19}
$$

and

$$
\Phi(k) = 0
$$

$$
\left.
\begin{aligned}
w(z) &= \begin{cases} w_1 \left[1 + D \cos\left(\dfrac{\pi z}{l}\right)\right] & \text{for } -\dfrac{l}{2} < z < \dfrac{l}{2} \\ 0 & \text{elsewhere} \end{cases} \\
S(k) &= \frac{1}{2\pi} \int_{-l/2}^{+l/2} \left[1 + D \cos\left(\pi \frac{z}{l}\right)\right] e^{-ikz}\, dz \\
&= \frac{1}{\pi k} \sin \frac{kl}{2} \left(1 + \frac{D\pi k}{l} \cot \frac{\frac{kl}{2}}{\frac{\pi^2}{l^2} - k^2}\right)
\end{aligned}
\right\}
\tag{B20}
$$

and

$$
\Phi(k) = 0
$$

$$
\left.
\begin{aligned}
w(z) &= w_1\left[1 + D\left(1 - \frac{2}{l}\,|x|\right)\right] \qquad -\frac{l}{2} < z < \frac{l}{2} \\
&= 0 \qquad \text{elsewhere} \\
D(k) &= \frac{\sin \frac{kl}{2}}{\pi k}\left(1 - \frac{2D}{k}\cot\frac{kl}{2}\right)
\end{aligned}
\right\}
\tag{B21}
$$

and

$$
\Phi(k) = 0
$$

$$
\left.
\begin{aligned}
w(z) &= w_{o,1}\left(1 - \frac{z}{l}\right) \qquad \text{for } 0 < z < l \\
&= 0 \qquad \text{elsewhere} \\
S(k) &= |S(k)|\,e^{i\Phi(k)} \\
|S(k)| &= \frac{1}{\sqrt{2}\,\pi k}\left[\frac{1 - \cos kl}{(kl)^2} - \frac{\sin kl}{kl} + \frac{1}{2}\right]^{1/2} \\
\tan \Phi(k) &= \frac{\sin kl - kl}{1 - \cos kl}
\end{aligned}
\right\}
\tag{B22}
$$

Formulas for M and L for the analyzed function $w_1(z)$ are as follows:

$$
w_1(z) = \text{const}
$$

$$
w_2 = \text{const throughout}
$$

$$
M_{1,2} = 8\mu_o abw_1w_2 \int_0^\infty I_1(kb)K_1(ka) \sin\frac{kl_1}{2} \sin\frac{kl_2}{2} \cos kx \frac{dk}{k^2}
\tag{B23}
$$

where

$a > b$; x is distance between centers of 1 and 2

$$w_1(z) = w_1\left(1 + D\cos\frac{\pi}{l}z\right) \quad \text{for } -\frac{l}{2} \leq z \leq \frac{l}{2}$$

$$M_{1,2} = 8\mu_o abw_1w_2 \int_0^\infty \left[1 + D\frac{\pi}{l_1}\frac{\cot\frac{kl_1}{2}}{\left(\frac{\pi^2}{l_1^2} - k^2\right)}\right]\sin\frac{kl_1}{2}\sin\frac{kl_2}{2} I_1(kb)K_1(ka)\cos kx\,\frac{dk}{k^2} \tag{B24}$$

where

$a > b$; x is distance between centers of 1 and 2

$$L_1 = 8\mu_o a^2w_1^2 \int_0^\infty \left(1 + D\frac{\pi}{l_1}\frac{k\cot\frac{kl_1}{2}}{\frac{\pi^2}{l_1^2} - k^2}\right)^2 I_1(ka)K_1(ka)\sin^2\frac{kl_1}{2}\frac{dk}{k^2} \tag{B25}$$

$$w(z) = w_1\left[1 + D\left(1 - \frac{2}{l_1}|z|\right)\right]$$

$$M_{1,2} = 8\mu_o abw_1w_2 \int_0^\infty \left[1 + \frac{2D}{kl_1}\left(\csc\frac{kl_1}{2} - \cot\frac{kl_1}{2}\right)\right]$$

$$\times I_1(kb)K_1(ka)\sin\frac{kl_1}{2}\sin\frac{kl_2}{2}\cos kx\,\frac{dk}{k^2} \tag{B26}$$

where

$a > b$

$$L_1 = 8\mu_0 a^2 w_1^2 \int_0^\infty \left[1 + \frac{2D}{k l_1}\left(\csc\frac{k l_1}{2} - \cot\frac{k l_1}{2}\right)\right]^2 I_1(ka)K_1(ka)\sin^2\frac{k l_1}{2}\,\frac{dk}{k^2} \tag{B27}$$

$$w(z) = w_{1,0}\left(1 - \frac{z}{l_1}\right) \quad \text{for } 0 < z < l_1$$

$$M_{1,2} = 8\mu_0 abw_{1,0}w_2 \int_0^\infty f(k l_1)I_1(kb)K_1(ka)\sin\frac{k l_2}{2}\cos\left[kx + \Phi(k)\right]\frac{dk}{k^2} \tag{B28}$$

where

$a > b$; x is distance between $x = 0$ on coil 1 and center of coil 2

$$L_1 = 8\mu_0 a^2 w_{1,0}^2 \int_0^\infty \frac{f(k l_1)}{k^2} I_1(ka)K_1(ka)\sin\frac{k l_1}{2}\cos\left[\frac{k l_1}{2} + \Phi(k)\right]dk$$

$$- 4\mu_0 a^2 w_{1,0}^2 \int_0^\infty \frac{f(k l_1)}{k^2} I_1(ka)K_1(ka)\sin\left[k l_1 + \Phi(k)\right]dk$$

$$+ 8\mu_0 a^2 w_{1,0}^2 \int_0^\infty \frac{f(k l_1)}{k l_1} I_1(ka)K_1(ka)\sin\frac{k l_1}{2}\sin\left[\frac{k l_1}{2} + \Phi(k)\right]\frac{dk}{k^2} \tag{B29}$$

$$f(k l_1) = \frac{1}{\sqrt{2}}\left[\frac{1}{2} + \frac{1 - \cos k l_1}{(k l_1)^2} - \frac{\sin k l_1}{k l_1}\right]^{1/2} \tag{B30}$$

$$\tan\Phi(k l_1) = \frac{\sin k l_1 - k l_1}{1 - \cos k l_1} \quad \text{for } -\frac{\pi}{2} \leq \Phi \leq 0 \tag{B31}$$

REFERENCES

1. Panofsky, W. K. H.; and Phillips, M.: Classical Electricity and Magnetism. Addison-Wesley Pub. Co., 1955, p. 138.

2. Smythe, W. R.: Static and Dynamic Electricity. Second Ed., McGraw-Hill Book Co., Inc., 1950, p. 267.

"*The aeronautical and space activities of the United States shall be conducted so as to contribute . . . to the expansion of human knowledge of phenomena in the atmosphere and space. The Administration shall provide for the widest practicable and appropriate dissemination of information concerning its activities and the results thereof.*"

—NATIONAL AERONAUTICS AND SPACE ACT OF 1958

NASA SCIENTIFIC AND TECHNICAL PUBLICATIONS

TECHNICAL REPORTS: Scientific and technical information considered important, complete, and a lasting contribution to existing knowledge.

TECHNICAL NOTES: Information less broad in scope but nevertheless of importance as a contribution to existing knowledge.

TECHNICAL MEMORANDUMS: Information receiving limited distribution because of preliminary data, security classification, or other reasons.

CONTRACTOR REPORTS: Technical information generated in connection with a NASA contract or grant and released under NASA auspices.

TECHNICAL TRANSLATIONS: Information published in a foreign language considered to merit NASA distribution in English.

TECHNICAL REPRINTS: Information derived from NASA activities and initially published in the form of journal articles.

SPECIAL PUBLICATIONS: Information derived from or of value to NASA activities but not necessarily reporting the results of individual NASA-programmed scientific efforts. Publications include conference proceedings, monographs, data compilations, handbooks, sourcebooks, and special bibliographies.

Details on the availability of these publications may be obtained from:

SCIENTIFIC AND TECHNICAL INFORMATION DIVISION

NATIONAL AERONAUTICS AND SPACE ADMINISTRATION

Washington, D.C. 20546